Electrolytic Recovery of Metals from Lithium Battery Cathodes in Moisture-Tolerant Molten Hydroxide Salt

Timothy Lichtenstein[1*], Jarrod Gesualdi[1], Sarah A. Stariha[1+], and Colin E. Moore[1+]

[1]Chemical and Fuel Cycle Technologies Division, Argonne National Laboratory, Lemont, IL 60439, United States

[+]Current Address: Honeywell UOP, Des Plaines, IL, 60016, United States

Author Email Addresses:

tlichtenstein@anl.gov, jgesualdi@anl.gov, sstariha@anl.gov, cmoore@anl.gov

Corresponding Author:

[*]E-mail: tlichtenstein@anl.gov, Tel: 630-252-5893, ORCiD: 0000-0002-4739-9907

KEYWORDS: Molten salts, battery recycling, electrodeposition

ABSTRACT

Lithium-ion battery recycling offers an opportunity to develop innovative technologies to close the loop on the battery materials cycle and increase the resilience of the battery supply chain. Here we demonstrate a two-step pyroelectrochemical method for producing mixed-metals from lithium-ion cathodes in a molten hydroxide salt. Mixed metal oxides in the form of insoluble lithium-ion cathode materials of $LiNi_{0.6}Mn_{0.2}Co_{0.2}O_2$ and spent lithium-ion battery materials (black mass) were electrochemically reduced to a soluble form and dissolved into a molten hydroxide salt bath. Electrochemical characterization of the process salt indicated accumulation of dissolved transition metals in the salt. A separate cathode was used to produce alloys of Ni, Mn, and Co electrochemically from the dissolved lithium-ion cathode materials. Characterization by scanning electron microscopy fitted with an energy dispersive X-ray spectrometer showed transition metals present in the cathode materials were recovered at the separate cathode. This approach represents a scalable, low temperature pyroelectrochemical process that can potentially reduce the cost and close the loop of battery cathode recycling.

1. INTRODUCTION

Demand for lithium-ion batteries and the critical metals (Li, Ni, and Co) from which they are manufactured is increasing globally[1], with many countries increasing their demand as more electric vehicles are purchased by consumers[2]. Recycling materials from spent batteries is a potential route for meeting that demand[2]. Commercialized battery recycling processes are based upon pyrometallurgical, hydrometallurgical, or a combination of the two routes to recover critical battery materials[3]. Existing commercial pyrometallurgical processes traditionally use high temperatures (>1000 °C), which require high-purity reagents, and use coke as a reductant which makes the process expensive and CO_2-intensive[3]. We seek to develop a pyroelectrochemical process that lowers the required temperatures and emissions needed for extraction of critical materials from lithium-ion batteries with a smaller carbon footprint than conventional pyrometallurgical routes. Here we demonstrate a pyroelectrochemical process that uses low melting temperature, moisture-tolerant molten hydroxide salts to electrochemically produce metals from lithium-ion batteries and the mixture of recycled battery materials called black mass.

Electrochemical routes for recovering metals from lithium-ion batteries are most often developed for extraction of metals from hydrometallurgical solutions[4]. In contrast, there are a small number of investigations into the direct extraction of metals from lithium-ion batteries and these studies have been focused on the extraction of cobalt[5,6]. Molten salts have been used extensively in the recovery of a variety of metals including lithium and may be a suitable electrolyte to recover metals from lithium-ion batteries[7]. For recycling of lithium-ion batteries, molten carbonate salts have been successfully employed to recover the Co present in $LiCoO_2$[6], but the operating temperature of these melts are high, approximately 750 °C, which increases the costs associated with the molten carbonate process[6]. Alternative well-studied molten salts

(e.g.,LiCl-KCl, FLiNaK, $CaCl_2$, etc.) that melt at lower temperatures are sensitive to potential uncontrolled moisture impurities and may degrade in the presence of moisture (e.g., formation of HF in molten fluoride salts[7]). Alternatively, LiCl has shown the capability to deoxygenate metal oxides (electrochemically reduce) in the presence of moisture[8]. This process requires control of the moisture content dissolved in the melt at temperatures higher than 600 °C to enable deoxygenation of transition metal oxides by the production of reductive hydrogen at the surface of the transition metal oxide[8].

Molten hydroxide salts are a moisture-tolerant, oxyanion conducting electrolyte system suitable for electrochemical extraction[9]. This water tolerance is unique among molten salts and enables electrochemistry with oxyanions through the Lux-Flood acid-base equilibrium:

$$2OH^- \leftrightarrow H_2O + O^{2-} \quad (1)$$

in which water is the oxoacid and accepts oxyanions to form the hydroxide ion. This reaction allows for electrochemistry of oxides to be performed in hydroxide melts. For example, pure molten NaOH has been used to electrochemically deoxygenate transition metals[10–13] and molten LiOH-KOH has been used as a solvent media to electrochemically deposit $LiCoO_2$ and $LiMnO_2$ [14]. The deoxygenation of metals and electrodeposition of lithiated transition metal oxides (lithium-ion cathode material) in molten hydroxide salts suggests that lithium-ion battery cathodes can be electrochemically deoxygenated to extract precious transition metals using molten hydroxide salts. However, the decomposition of dissolved moisture limits the cathodic polarization of the salt preventing efficient deposition of metal from the salt [14], necessitating methods to deal with moisture impurities in order to effectively produce metals from the melt. Furthermore, black mass contains additional impurities such as copper, aluminum, and carbon from current collectors and binders that would need to be tolerated. Here, we present our pyroelectrochemical approach

for electroreducing and extracting metals from lithium-ion battery cathodes and black mass using the LiOH-KOH eutectic under both moist and dehydrated conditions.

2.EXPERIMENTAL

All tests were performed in a stainless-steel vacuum test chamber placed within a Ventura melt bench top furnace. Cathode materials tested were $LiNi_{0.6}Mn_{0.2}Co_{0.2}O_2$ (NMC 622, Targray) or black mass provided by ReCell. The black mass contained 2.16 wt % Al, 6.37 wt % Co, 3.85 wt % Cu, 0.19 wt % Fe, 3.46 wt % Li, 6.01 wt % Mn, 0.03 wt % Na, 16.79 wt % Ni, 0.35 wt % P, 0.25 wt % S based upon elemental characterization provided by ReCell. Test pellets of NMC622 were fabricated by hydraulically pressing NMC622 powder at 3 tons of pressure and then calcining for 5 h at 825 °C. No binder was added to the NMC622. Black mass electrodes were pressed at 3 tons of pressure and were not further heated as they were mechanically robust as-pressed.

The experimental setup is shown schematically in Figure 1 and consisted of an alumina crucible containing LiOH-KOH eutectic synthesized from anhydrous 99.9 % LiOH and 99.98 % trace metals KOH for the NMC622 tests and from anhydrous 98 % LiOH and 85 % KOH for the black mass tests. An electrolyte of LiOH-KOH was chosen due to its low melting temperature eutectic (225 °C) [15], capability for production of insoluble lithiated transition metal oxides [14], inherent moisture tolerance, and potential for the recovery of Li metal using electrolysis [16]. Working electrodes consisted of a tungsten wire, tungsten rod, stainless-steel plate, or a stainless-steel basket filled with calcined $LiNi_{0.6}Mn_{0.2}Co_{0.2}O_2$ (NMC622) or black mass pellets. A graphite rod served as counter electrode, and a tungsten wire served as a quasi-reference electrode as no well-characterized reference electrode exists at present for molten LiOH-KOH salts. The loaded test vessel was sealed within an inert atmosphere glovebox (maintained at < 0.1 ppm O_2 and < 0.5 ppm H_2O), removed, and transferred to a bench top furnace. The assembled cell was dried under

a vacuum of 120 millitorr at either 200 °C or 280 °C overnight before testing under an ultra-high purity argon purge atmosphere. Temperature was monitored using a K-Type thermocouple placed external to the crucible at the salt level. The temperature of the test vessel was maintained at 280 ± 5°C during experimentation. The electrochemical cells were controlled by a Gamry Interface 5000E potentiostat. Recovered products from the cathode basket were imaged and characterized by scanning electron microscopy (Hiatchi 3400 with Bruker Nano GmbH XFlash detector 610) with energy dispersive X-ray spectroscopy (SEM-EDS).

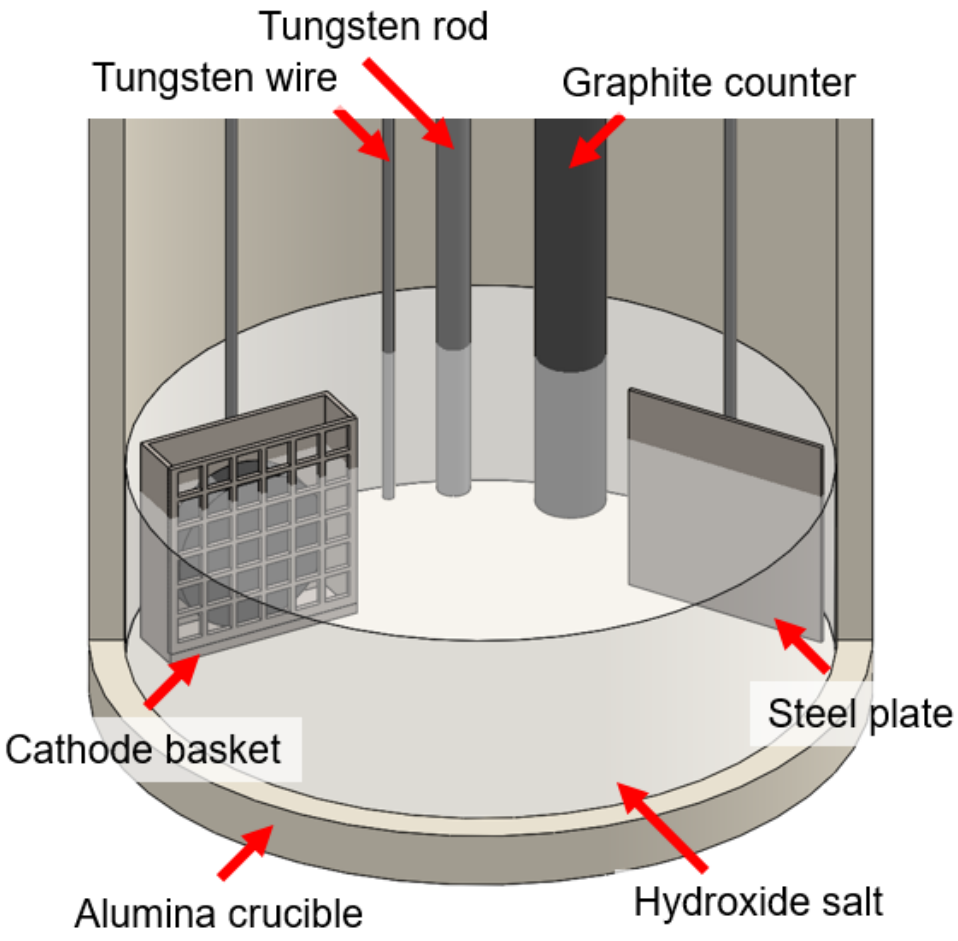

Figure 1. Schematic electrochemical cell used for testing consisting of a cathode basket with pressed test pellets, a steel plate, a tungsten rod, a tungsten wire reference electrode, a graphite counter electrode housed within an alumina crucible.

3.RESULTS

3.1 Electrolyte Selection and Treatment

Although molten hydroxide salts are tolerant to moisture, the presence of moisture limits the control of electrochemical reactions as the decomposition of water is the typical cathodic limit to the electrochemical window. As such, three methods to dry the salt were evaluated: by first drying a test salt as a solid at 200 °C, by drying the salt in the liquid state at 280 °C, and by drying the salt electrolytically. Electrochemical investigation was performed using a tungsten wire to evaluate the changes to the moisture content under the three drying conditions. The cyclic voltammogram (CV) in Figure 2a for the solid drying (red) has an anodic feature associated with the dissolution of tungsten (Feature 1, approximately 0.1 V vs. W wire) and a large cathodic feature (2, approximately -0.25 V vs. W wire) indicative of the decomposition of the dissolved water [14,17]. The salt used in a second cell was dried by placing the salt under vacuum, then melting the salt under vacuum and leaving it overnight. CVs obtained in the liquid-dried melt (Figure 2a, black curve) show the current of the water decomposition feature is significantly decreased (Feature 2, Figure 2a) and an additional cathodic feature (Feature 3, Figure 2a, black curve) is revealed and is likely correlated with the production of alkali metal. If we consider the formation energy, ΔG_f, of the constituent salt hydroxides then the deposited alkali metal is likely K as the formation energy of KOH ($K + 0.25\ O_2 + 0.5\ H_2O = KOH$, $\Delta G_f = -231.2$ kJ mol^{-1} at 280 °C) is less negative (less electrochemically stable) than the LiOH ($Li + 0.25\ O_2 + 0.5\ H_2O = LiOH$, $\Delta G_f = -290.8$ kJ mol^{-1} at 280 °C) [15]. Empirical identification of the alkali metal generated was not performed in the course of this work.

A separate test was performed to evaluate the effectiveness of electrolysis as a method for removing moisture from the melt. Electrolysis is an industrially relevant process that may be a

more attractive treatment method for drying hydroxide salts than using a vacuum. Electrolysis was tested by subjecting a solid-dried LiOH-KOH melt to 6 Ah of electrolysis at 500 mA through two graphite electrodes. Linear sweep voltammograms (LSVs) performed with a 1 A cut-off current before and after electrolysis are shown in Figure 2b. The current of the reaction associated with dissolved moisture (Feature 2, Figure 2b) decreased in magnitude and the alkali metal production reaction (Feature 3, Figure 2b) was achieved during LSVs after the 6 Ah electrolysis test. The dissolved moisture undergoes the following reaction mechanism at the cathode during electrolysis[18]:

$$2H_2O + 2e^- \rightarrow 2OH^- + H_2 \quad (2)$$

The hydroxide anions react at the anode to form gaseous oxygen and steam through the following reaction[18]:

$$6OH^- \rightarrow 3H_2O + 1.5O_2 + 6e^- \quad (3)$$

Anodically generated moisture may re-dissolve into the melt and lower the overall efficiency of removing moisture by electrolysis. However, our results show that there is a net moisture decrease in the melt and that it is possible to eliminate moisture by electrolysis.

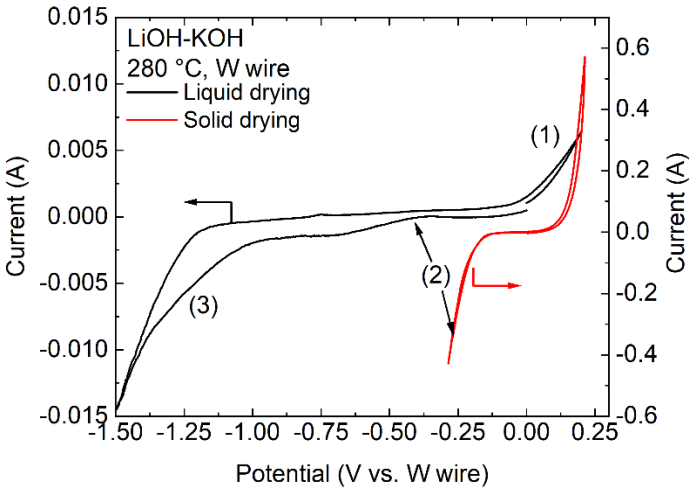

(a)

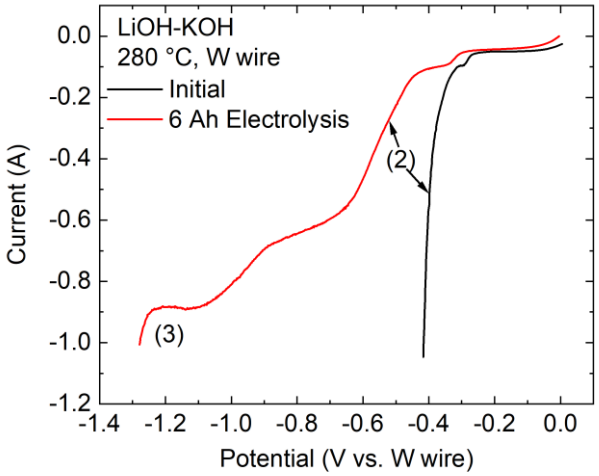

(b)

Figure 2. (a) CVs of a tungsten wire in the LiOH-KOH after drying the salt under vacuum as a liquid (black) and as a solid state (red) and (b) LSVs of a tungsten wire in a solid-dried LiOH-KOH melt before (black) and after (red) electrolyzing for 6 Ah.

3.2 Electrolysis of NMC 622 under moist and dry conditions

The electrolysis was performed to assess the recovery of metal from lithium-ion cathode materials. Electrochemical characterization of the cathode materials and the salt was performed in both moist and dry electrolytes using calcined NMC622 charged in a stainless-steel basket to enhance electrical contact with the cathode basket and tungsten electrodes. Figure 3a shows cyclic voltammograms (CVs) of a NMC622 charged basket in moist and dried electrolyte overlain. The moist electrolyte shows the onset of a cathodic reaction at approximately -0.2 V vs. W wire, similar to what was observed in a moist melt on a tungsten wire (Figure 2a, red curve). CVs of the dried electrolyte show additional cathodic features at approximately -0.4 V vs. W wire and a rapid increase in current at potentials more negative than -0.56 V vs. W wire. The reaction at approximately -0.2 V vs. W wire in the moist salt is the reduction of moisture on the steel basket whereas the more negative features are associated with the reduction of the NMC622 material.

Electrolysis was performed with the calcined NMC622 pellets in moist and dry electrolytes and the results are shown in Figure 3b and Figure 3c, respectively. During electrolysis, the potential measured in the moist electrolyte is noisy. This is a characteristic feature of gas evolution reactions and is expected as hydrogen gas is produced during water reduction (Reaction 2). The pellet in dry electrolyte was held at -1.4 V vs. W wire to perform the NMC622 reduction but prevent the formation of excess alkali metal. A CV performed before and after electrolysis on a tungsten electrode in a dry salt shows an increase in the current associated with the moisture reduction (Feature 2, Figure 3d) of the salt due to Reaction 3 occurring at the anode during electrolysis of the NMC622 pellet. Several additional features (Features 4–7, Figure 3d) appear at voltages more negative of the reduction potential of dissolved moisture and the -0.56 V vs. W wire feature of the bulk NMC622 from Figures 3a, indicating NMC622 reduced to a soluble form during electrolysis.

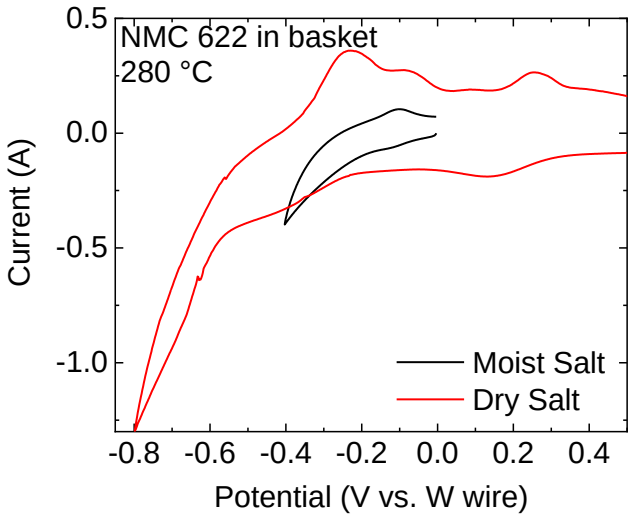

(a)

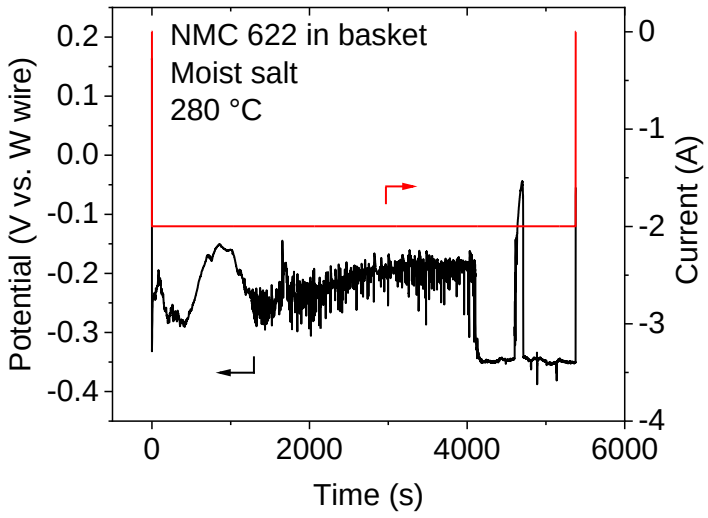

(b)

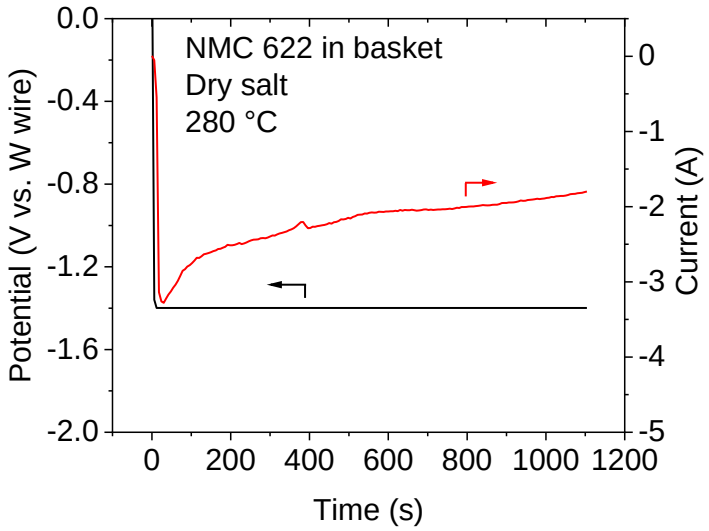

(c)

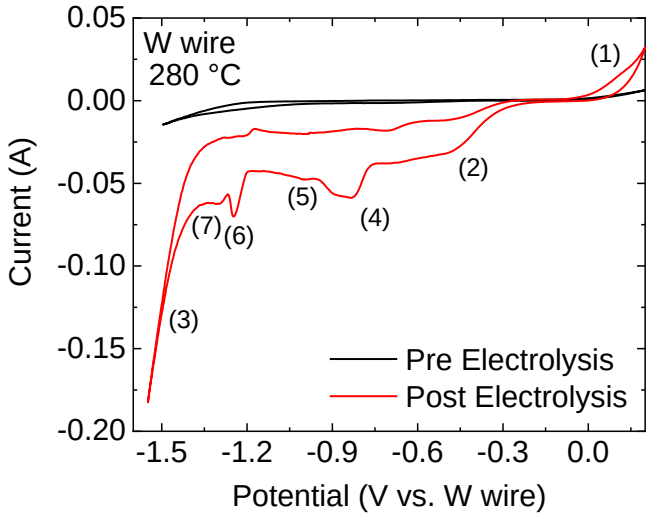

(d)

Figure 3. (a) CVs of an NMC622 pellet within a stainless-steel cathode basket in a moist salt (black) and dry salt (red), (b) Electrochemical response of a calcined NMC622 during electrolysis in a moist salt, (c) Electrochemical response of a calcined NMC622 during electrolysis in a dry salt, and (d) CV of a W wire in a dry salt before (black) and after (red) electrolyzing NMC622 into the melt.

Figure 4a–c shows photographs of the as-calcined material prior to testing, after immersion in the melt for 16 hours, and after electrolysis, respectively. The photographs show the calcined pellet was only minimally deformed during immersion, but significantly deformed during electrolysis. This suggests that electrolysis greatly affects the structure of the calcined pellet and electrolysis may promote dissolution into the melt.

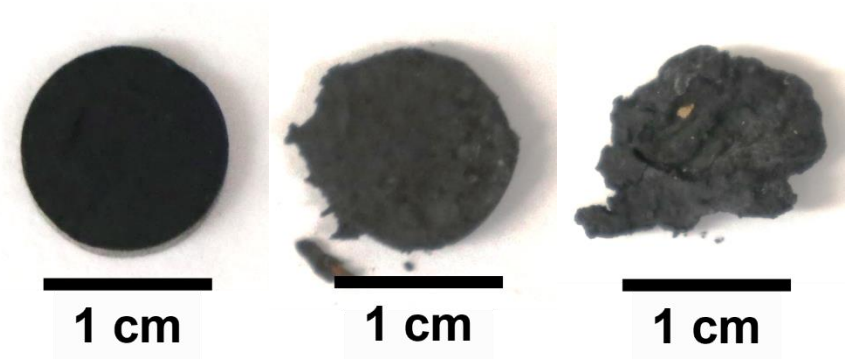

(a) (b) (c)

Figure 4. (a) Photograph of a calcined NMC622 pellet, (b) photograph of a calcined NMC622 pellet after immersion in a dry salt for 16 h, and (c) photograph of residual NMC622 recovered from a cathode basket after electrolysis in a dry salt.

Characterization of electrolysis products recovered from cathode baskets were performed and compared to commercial powdered NMC622 (Figure 5a). The electrolysis in dry electrolyte partially dissolved the NMC622 particle (Figure 5b), where the boundary between the dissolved and undissolved particle is marked by the red arrow. The EDS maps shown in Figure 5b confirms that the undissolved part of the particle still contains significant oxygen content and was not reduced to metal. Electrolysis in moist electrolyte led to the recovery of partially reduced NMC622 particles (Figure 5c) from the cathode basket after electrolysis. The recovered NMC622 are more porous in appearance than the feedstock NMC622. The EDS maps in Figure 5c show low

concentrations of oxygen in the recovered particulate. The electrolyte was examined before (Figure 6a) and after (Figure 6b) electrolysis with dry electrolytes and NMC622. The electrolyte changed colors from white to green indicating that some transition metals had dissolved into the melt during electrolysis. Similar observations occurred in both moist and dry conditions in this work. Furthermore, Zhang et al., observed a similar phenomenon. Their LiOH-KOH melt turned blue when soluble CoO was introduced and complexed as $Co(OH)_4^{2-}$[14].

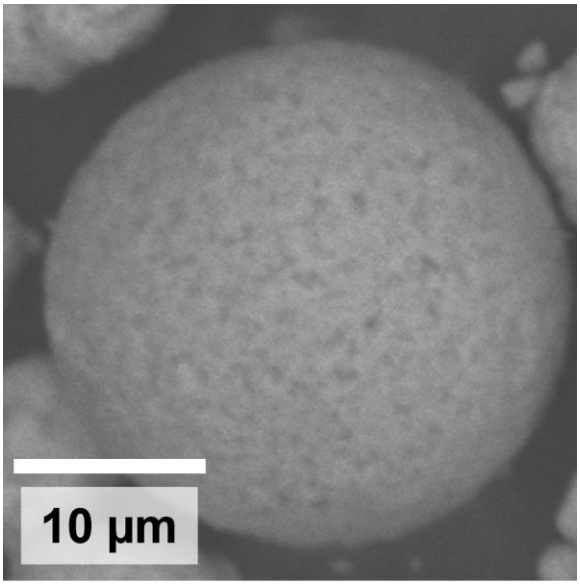

(a)

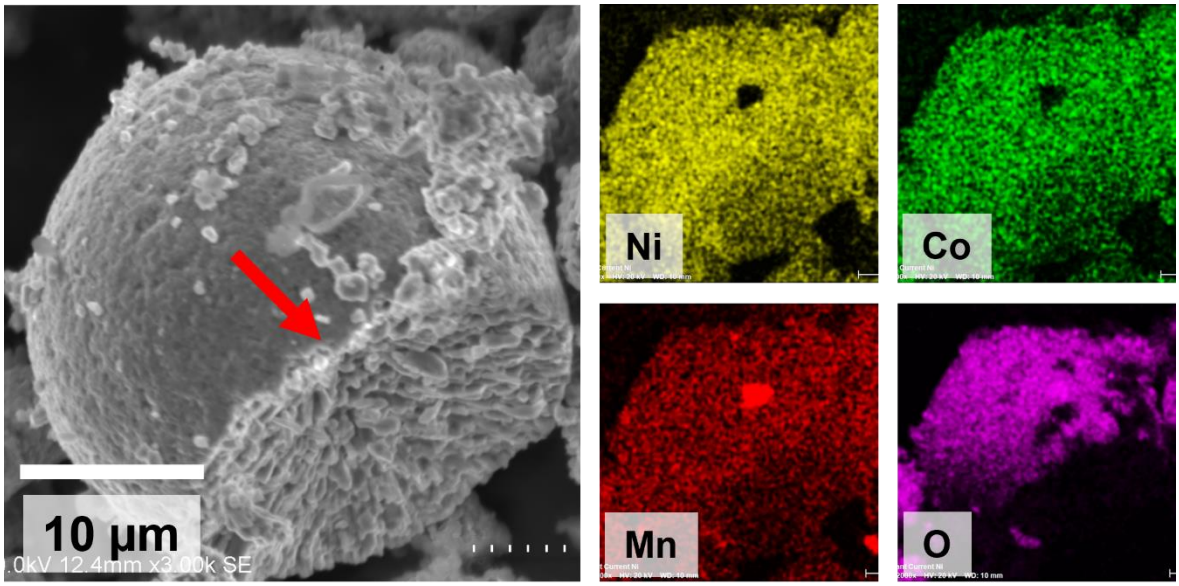

(b)

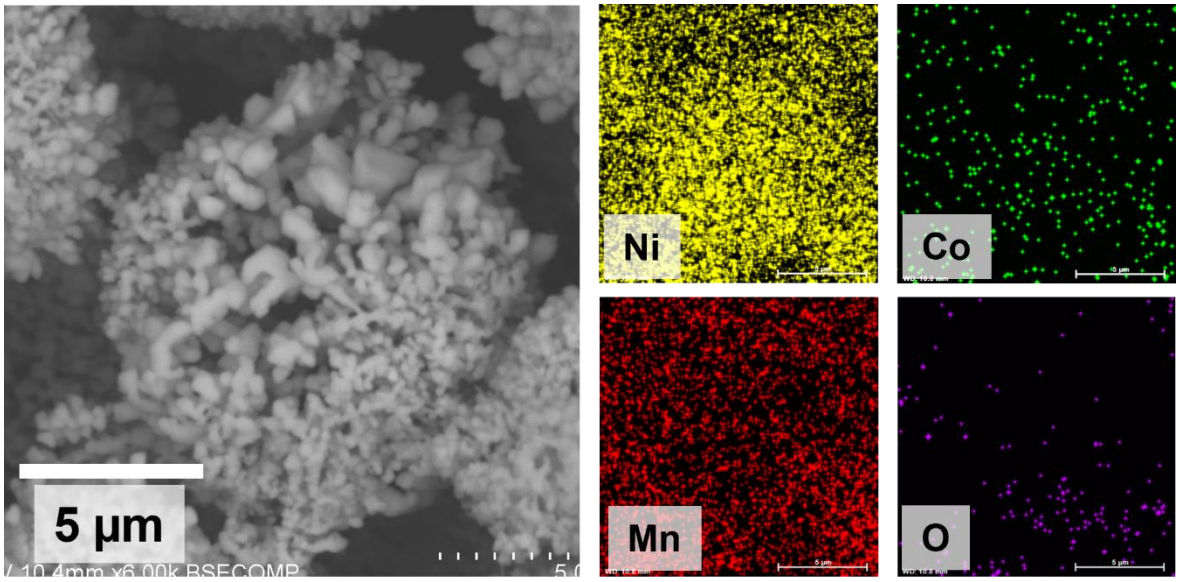

(c)

Figure 5 (a) SEM photomicrograph of feedstock NMC622, (b) SEM photomicrograph of partially dissolved NMC622 after electrolysis in a dry LiOH-KOH melt and EDS maps of partially dissolved NMC622 particle, (c) SEM photomicrograph of reduced NMC622 from moist LiOH-KOH and EDS maps of reduced NMC622 from moist LiOH-KOH.

(a) (b)

Figure 6. (a) Photograph of a fused LiOH-KOH salt, and (b) photograph of a fused LiOH-KOH after electrolysis of NMC 622 with a discarded basket fused to the top of the salt.

The observed dissolution of the lithiated transition metal oxides occurs due to an insoluble-soluble transition. Here, the insoluble cathode material dissolves (solubilizes) into the melt under reducing electrochemical conditions, shown in Reaction (4) for a generic lithiated oxide; any lithium-ion cathode will likely reduce by this mechanism:

$$LiAO_2(s) + e^- \rightarrow Li^+ + O^{2-} + AO\ (sol) \quad (4)$$

Where A is a transition metal (Ni, Mn, Co). The reduction process liberates the Li^+ and O^{2-} ions into the melt, while reducing the transition metal from 3^+ to 2^+ which is soluble in the melt[14]. The accumulated O^{2-} is then discharged at the anode as gaseous oxygen and steam through Reactions 1 and 3. The 2^+ valence transition metal may also oxidize at the anode to a soluble or insoluble 3^+ compound depending on moisture content and the transition metal of interest. For example Zhang et al., observed anodic $LiCoO_2$ deposition from moist salts and speculated that Co_3O_4 may anodically deposit but would be unstable in moist salts[14]. This may lower the overall efficiency of the metal recovery but further investigation into the electrochemical behavior of the individual dissolved transition metals is necessary and beyond the scope of the current work. The recovery of metallic particles in Figure 5c from cathode baskets in moist electrolytes suggests that the reduction of moisture to hydrogen at the surface of the NMC622 pellet further reduces some of the partially dissolved particles to their metallic form while accumulating the excess metal oxide materials (e.g., CoO and MnO) into the melt.

The solubilized metal oxides can be recovered electrolytically on a separate cathode. The recovery of the solubilized transition metal oxides as metal alloys in both moist and dry electrolyte was tested by electrolysis after reducing 2 g of NMC622 into the melt. A steel plate was used as the cathode for tests in dry salts and a tungsten rod was used for tests in moist salts, both were discharged at -2 A to electrolyze metals. The electrochemical signal for electrolysis is shown in

Figure 7a for the steel plate and Figure 7b for the tungsten rod. The average electrolysis potential for the steel plate was approximately -0.9 and for the tungsten rod was approximately -1.1 V vs W wire. Both were more negative than the moisture decomposition reaction, indicating removing moisture may not be necessary to recover metals from the melt but the presence of moisture may decrease the efficiency of the metals extraction.

Figure 7c is the SEM photomicrograph of the dry salt electrolysis product and the EDS mapping for the sample. The backscattered electron photomicrograph shows bright fine metallic needles (Figure 7c, red arrow) with significant entrained salt surrounding the needles (Figure 7c, blue arrow). The EDS spectra show nickel, cobalt, and manganese were recovered as fine needles with significant oxygen present due to the entrained salt and high surface area of the fine metallic particles. Figure 7d shows the SEM photomicrograph and EDS spectra of the electrolysis product on a tungsten electrode from a moist electrolyte, respectively. The product morphology was fine and contained nickel, cobalt, and manganese from the NMC622 and oxygen due to the fine morphology of the metallic particles. Optimization of deposition parameters such as applied potential and current density will be necessary moving forward to obtain value added alloy materials.

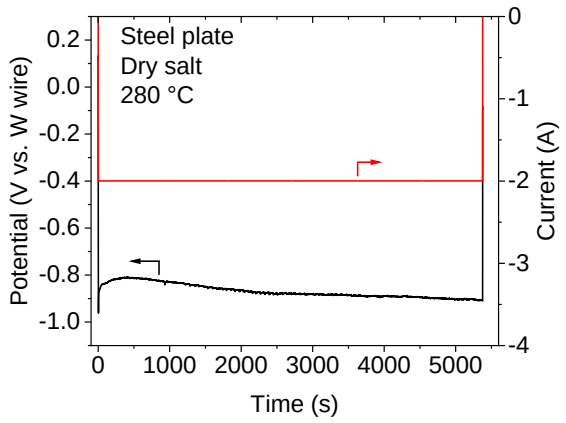

(a)

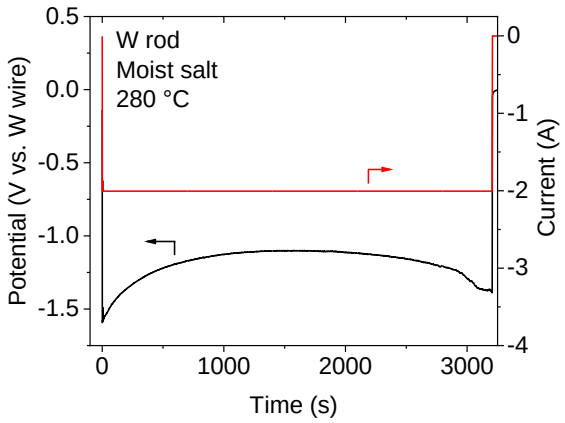

(b)

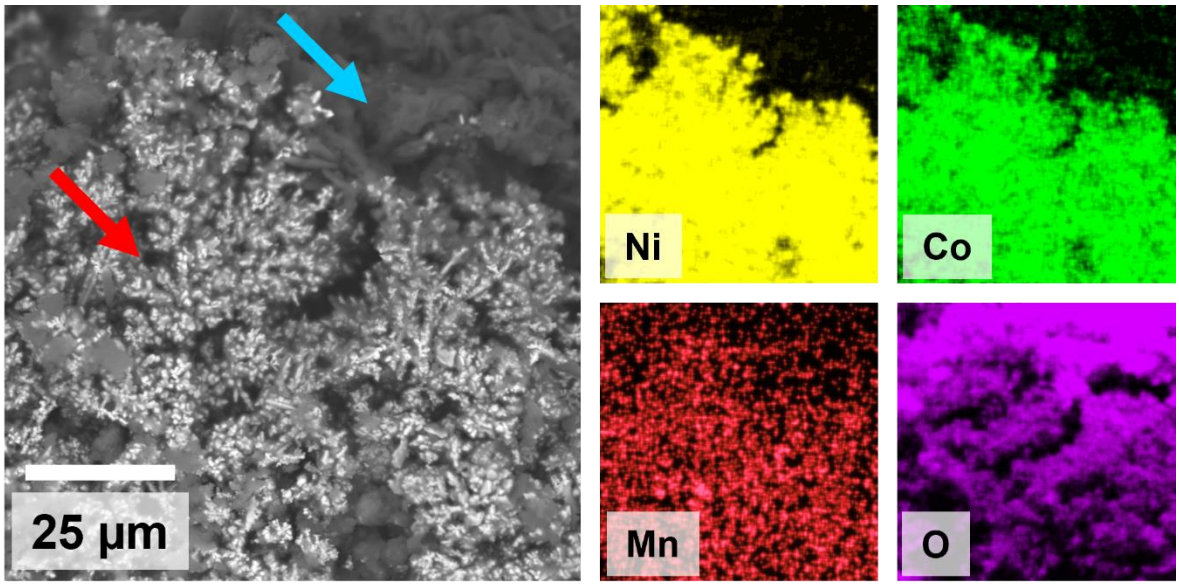

(c)

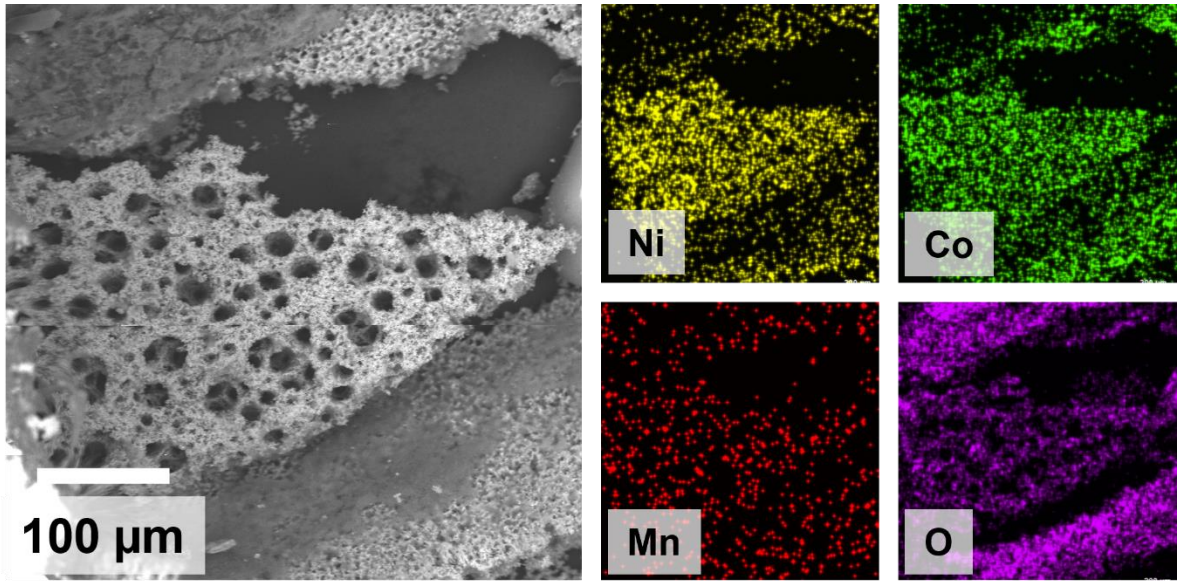

(d)

Figure 7. (a) Electrochemical signal during electrolysis onto a steel cathode from a dry LiOH-KOH melt, (b) electrochemical signal during electrolysis onto a W rod electrode from a moist LiOH-KOH melt (c) SEM photomicrograph of an alloy electrolyzed from a dry LiOH-KOH melt , and EDS mapping of alloy recovered from a dry LiOH-KOH melt, (d) SEM photomicrograph of

an alloy electrolyzed from a moist LiOH-KOH melt and EDS mapping of the alloy recovered by electrolysis in a moist LiOH-KOH melt.

3.3 Extraction of transition metals in the presence of impurities from black mass

A pyroelectrochemical recycling process using molten hydroxide salt would be required to function in the presence of impurities associated with black mass materials. The reduction-electrolysis was performed with black mass acquired from ReCell to test the applicability of molten hydroxides for reduction-electrolysis using real spent battery materials. Lower purity LiOH and KOH were selected for the black mass demonstration to reflect purities that are relevant for scale-up. Figure 8a and 8b show a pressed black mass pellet before and after electrolysis in a dry low purity melt, respectively. The black mass pellet lost its structure like the NMC622 pellet (Figure 4c) and the electrolyte changed from white to black (Figure 8c) during testing due to the accumulation of soluble species or fine carbon particles from the black mass electrode. Figure 8d shows the electrochemical response of a stainless-steel cathode basket containing a black mass pellet discharged at -0.25 A to prevent the potentials from rapidly reaching the alkali metal production potentials (-1.4 V vs. W wire). The potential measurements of the black mass shows three distinct regions numbered 1, 2, and 3 with their boundaries marked by blue vertical lines. The first region has an average potential of about -0.72 V vs. W wire, the potentials of the second region become more negative from -0.72 to -1.23 V vs. W wire, and the potentials of the third region decreases to a minimum potential of -1.8 V vs. W wire. We speculate that the reactions occurring in region 1 correspond to the reactions 4 and 5 presented in Figure 3d, the reactions in region 2 correspond to reactions 6 and 7 in Figure 3d, and the reactions in region 3 correspond to the generation of reduced alkali metals at the black mass electrode.

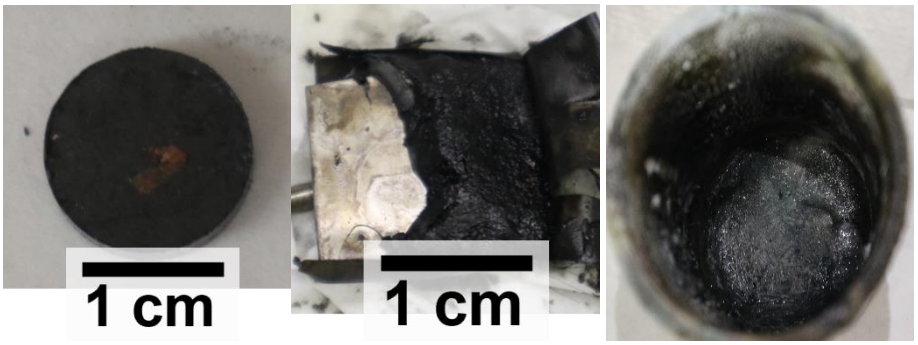

(a) (b) (c)

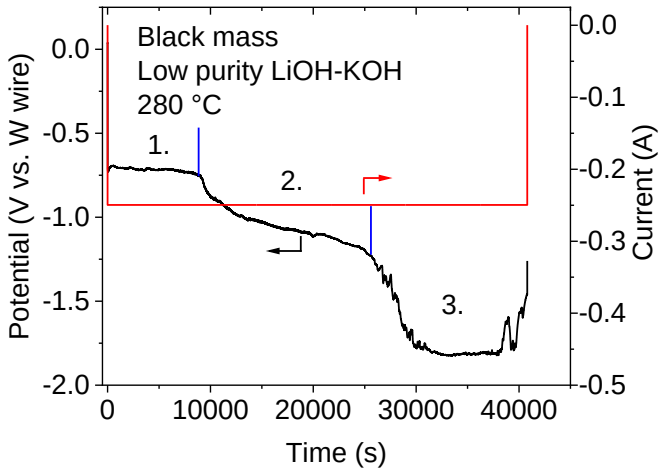

(d)

Figure 8. (a) Photograph of a pressed black mass pellet, (b) black mass material recovered from a cathode basket after electrolysis in a dry low purity LiOH-KOH melt. (c) photograph of the LiOH-KOH melt after electrolysis of black mass, (d) electrochemical signal of a black mass electrode during electrolysis in a dry low purity LiOH-KOH melt.

A stainless-steel plate was used to electrolyze the metals from the melt under constant current conditions of -1 A in Figure 9a. The potential continuously decreased under discharge from -1.39 to -2.1 V vs. W wire during electrolysis, in contrast to the stepwise potentials seen during the electrolysis of the black mass pellet. A photograph of the steel plate cathode with the recovered product is shown in Figure 9b, significant material was recovered from the melt on the

surface of the cathode. A SEM photomicrograph in Figure 9c shows the recovered product and the EDS X-ray mapping associated with it. The recovered product formed a plate structure and contained the metals Ni, Mn, Co, as well as Al and Cu metals from processed current collectors. Further investigation and optimization of the deposition parameters (i.e., current density, potentials) is necessary to control the metal alloy product composition and morphology. Nonetheless we have demonstrated that metals present as oxides or concomitantly in the battery recycling process can be recovered on a separate reducing cathode for further processing. Furthermore, recent work has demonstrated that molten hydroxide salts can be used to deposit Na-ion battery materials[19] by a similar mechanism as Li-ion battery materials[14], meaning that an appropriately designed molten hydroxide salt system could produce metal from both lithium-ion and sodium-ion batteries as feedstock.

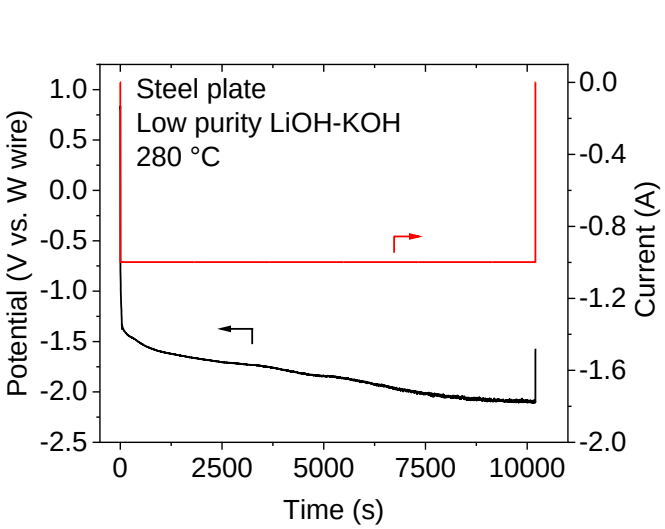

(a)

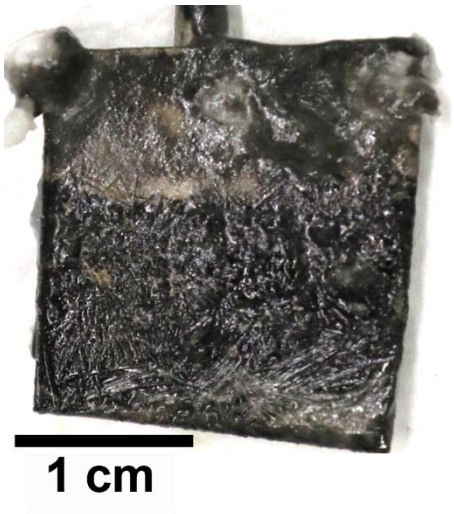

(b)

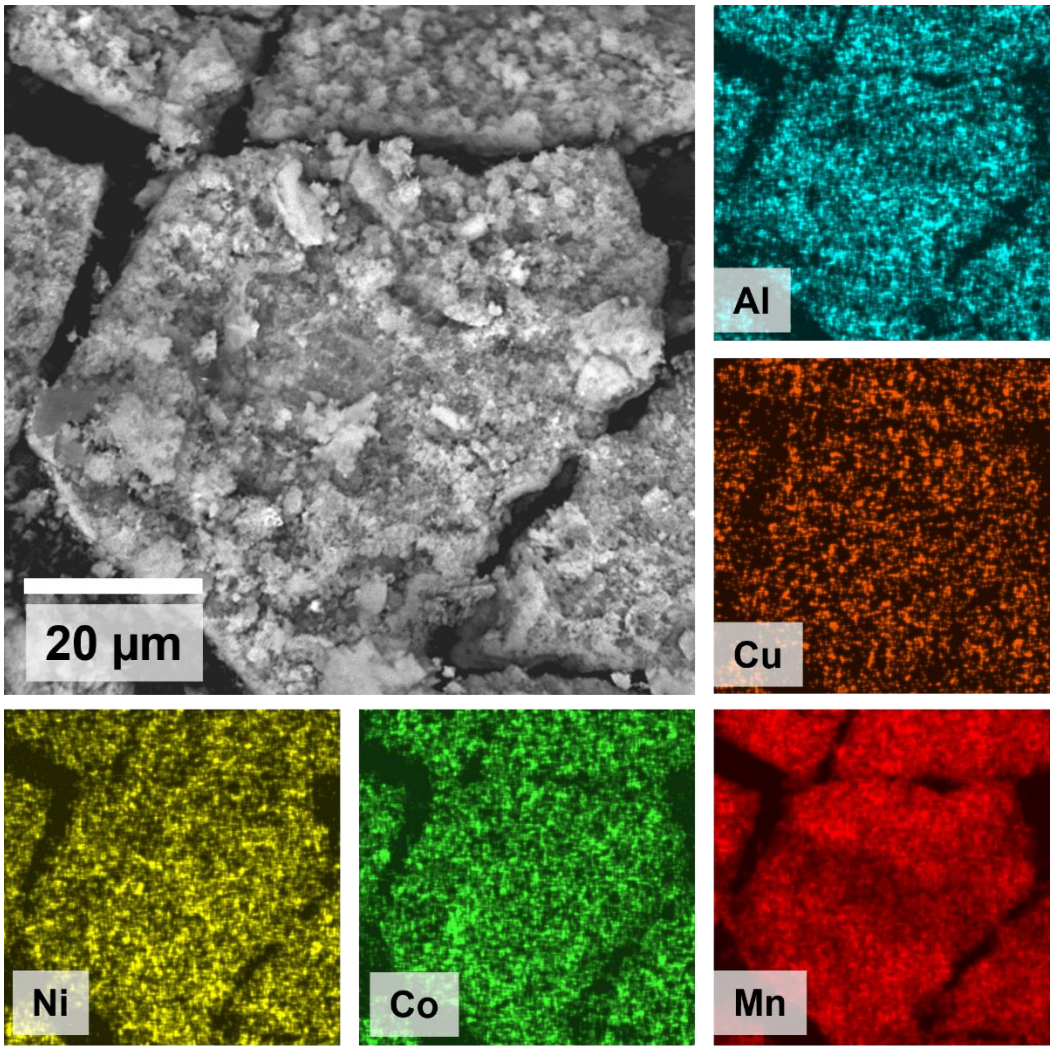

(c)

Figure 9. (a) electrochemical signal of a stainless-steel cathode during electrolysis of dissolved material from the dry low purity LiOH-KOH melt, (b) photograph of the recovered steel plate after electrolysis in the dry low purity LiOH-KOH melt, (c) SEM photomicrograph of the material recovered on the steel plate and EDS mapping of the material recovered on the steel cathode.

Conclusions

Electrolysis in a molten LiOH-KOH electrolyte was carried out to reduce NMC622 and black mass to metal constituents. We showed that NMC622 and black mass undergo an electrolytic reduction to a soluble form in both moist and dry melts. Further testing indicated recovery of leached cathode material electrolytically as an alloy at a separate cathode. A large electrochemical feature associated with the decomposition of the salt (reduction of alkali ions to metal) suggests molten hydroxide salts can function as a one-pot process to recover all the transition metals from spent lithium-ion battery cathodes. Future testing will focus on identifying the alkali metal reduction, recovery efficiency of the metals, and selective separation of the transition metals during electrolysis. Our data suggest that pyroelectrochemical processing of cathode materials in molten LiOH-KOH salts may be a viable method to recover valuable metal components at temperatures and carbon emissions that are lower than conventional high temperature pyroprocessing of battery cathodes. Furthermore, the use of molten hydroxides to deoxygenate transition metals suggests that electrometallurgical processing of other battery cathode materials (e.g., $LiFePO_4$, Na-ion batteries, etc) in hydroxide salts is possible. Further optimization of this method may make pyroprocessing of battery cathode materials more economically viable and close the lifecycle of battery cathode materials.

CONFLICTS OF INTEREST

There are no conflicts to declare.

ACKNOWLEDGEMENTS

This work was conducted under the auspices of the US Department of Energy, Energy Efficiency and Renewable Energy Vehicle Technologies Office as part of the ReCell Battery R&D Center.

The submitted manuscript has been created by UChicago Argonne, LLC, Operator of Argonne National Laboratory ("Argonne"). Argonne, a U.S. Department of Energy Office of Science laboratory, is operated under Contract No. DE-AC02-06CH11357.

Author Contributions

Timothy Lichtenstein- Conceptualization, Methodology, Investigation, Formal Analysis, Supervision, Funding Acquisition, Data Curation, Project Administration, Writing-Original Draft. **Jarrod Gesualdi**- Data Curation, Investigation, Visualization, Validation, Writing-Review and Editing. **Sarah A. Stariha**- Data Curation, Investigation, Visualization, Writing-Review and Editing. **Colin E. Moore-** Investigation, Validation

REFERENCES

[1] D.L. Thompson, J.M. Hartley, S.M. Lambert, M. Shiref, G.D.J. Harper, E. Kendrick, P. Anderson, K.S. Ryder, L. Gaines, A.P. Abbott, The importance of design in lithium ion battery recycling-a critical review, Green Chem. 22 (2020) 7585–7603. https://doi.org/10.1039/d0gc02745f.

[2] E. Mossali, N. Picone, L. Gentilini, O. Rodrìguez, J.M. Pérez, M. Colledani, Lithium-ion batteries towards circular economy: A literature review of opportunities and issues of recycling treatments, J. Environ. Manage. 264 (2020). https://doi.org/10.1016/j.jenvman.2020.110500.

[3] B. Makuza, Q. Tian, X. Guo, K. Chattopadhyay, D. Yu, Pyrometallurgical options for recycling spent lithium-ion batteries: A comprehensive review, J. Power Sources. 491 (2021) 229622. https://doi.org/10.1016/j.jpowsour.2021.229622.

[4] J.J. Roy, S. Rarotra, V. Krikstolaityte, K.W. Zhuoran, Y.D.I. Cindy, X.Y. Tan, M. Carboni, D. Meyer, Q. Yan, M. Srinivasan, Green Recycling Methods to Treat Lithium-

Ion Batteries E-Waste: A Circular Approach to Sustainability, Adv. Mater. 34 (2022) 1–27. https://doi.org/10.1002/adma.202103346.

[5] D. il Ra, K.S. Han, Used lithium ion rechargeable battery recycling using Etoile-Rebatt technology, J. Power Sources. 163 (2006) 284–288. https://doi.org/10.1016/j.jpowsour.2006.05.040.

[6] J. Zhao, X. Qu, J. Qu, B. Zhang, Z. Ning, H. Xie, X. Zhou, Q. Song, P. Xing, H. Yin, Extraction of Co and Li2CO3 from cathode materials of spent lithium-ion batteries through a combined acid-leaching and electro-deoxidation approach, J. Hazard. Mater. 379 (2019) 120817. https://doi.org/10.1016/j.jhazmat.2019.120817.

[7] X. li Xi, M. Feng, L. wen Zhang, Z. ren Nie, Applications of molten salt and progress of molten salt electrolysis in secondary metal resource recovery, Int. J. Miner. Metall. Mater. 27 (2020) 1599–1617. https://doi.org/10.1007/s12613-020-2175-0.

[8] K. Xie, A.R. Kamali, Electro-reduction of hematite using water as the redox mediator, Green Chem. 21 (2019) 198–204. https://doi.org/10.1039/c8gc02756k.

[9] E. Gürbüz, E. Grépin, A. Ringuedé, V. Lair, M. Cassir, Significance of Molten Hydroxides With or Without Molten Carbonates in High-Temperature Electrochemical Devices, Front. Energy Res. 9 (2021) 1–10. https://doi.org/10.3389/fenrg.2021.666165.

[10] Z. Zhou, H. Jiao, J. Tu, J. Zhu, S. Jiao, Direct Production of Fe and Fe-Ni Alloy via Molten Oxides Electrolysis, J. Electrochem. Soc. 164 (2017) E113–E116. https://doi.org/10.1149/2.0881706jes.

[11] S. Wang, J. Ge, Y. Hu, H. Zhu, S. Jiao, Electrochemical reduction of iron oxide in molten sodium hydroxide based on a Ni0.94Si0.04Al0.02 metallic inert anode, Electrochim. Acta. 87 (2013) 148–152. https://doi.org/10.1016/j.electacta.2012.09.044.

[12] J. Ge, F. Zhang, H. Jiao, S. Jiao, Metallic Nickel Preparation by Electro-Deoxidation in Molten Sodium Hydroxide, J. Electrochem. Soc. 162 (2015) E185–E189. https://doi.org/10.1149/2.0811509jes.

[13] D. Tian, H. Jiao, J. Xiao, M. Wang, S. Jiao, The corrosion behavior of a Ni0.91Cr0.04Cu0.05 anode for the electroreduction of Fe2O3 in molten NaOH, J. Alloys Compd. 769 (2018) 977–982. https://doi.org/10.1016/j.jallcom.2018.08.073.

[14] H. Zhang, H. Ning, J. Busbee, Z. Shen, C. Kiggins, Y. Hua, J. Eaves, J. Davis, T. Shi, Y.T. Shao, J.M. Zuo, X. Hong, Y. Chan, S. Wang, P. Wang, P. Sun, S. Xu, J. Liu, P. V. Braun, Electroplating lithium transition metal oxides, Sci. Adv. 3 (2017) 1–9. https://doi.org/10.1126/sciadv.1602427.

[15] C.W. Bale, E. Bélisle, P. Chartrand, S.A. Decterov, G. Eriksson, A.E. Gheribi, K. Hack, I.H. Jung, Y.B. Kang, J. Melançon, A.D. Pelton, S. Petersen, C. Robelin, J. Sangster, P. Spencer, M.A. Van Ende, FactSage thermochemical software and databases, 2010-2016, Calphad Comput. Coupling Phase Diagrams Thermochem. 54 (2016) 35–53. https://doi.org/10.1016/j.calphad.2016.05.002.

[16] Z. Tang, X. Guan, Lithium Extraction from Molten LiOH by Using a Liquid Tin Cathode, J. Sustain. Metall. 7 (2021) 203–214. https://doi.org/10.1007/s40831-021-00339-1.

[17] M.H. Miles, Exploration of molten hydroxide electrochemistry for thermal battery applications, J. Appl. Electrochem. 33 (2003) 1011–1016. https://doi.org/10.1023/A:1026270119048.

[18] A. Cox, D.J. Fray, Mechanistic investigation into the electrolytic formation of iron from iron(III) oxide in molten sodium hydroxide, J. Appl. Electrochem. 38 (2008) 1401–1407. https://doi.org/10.1007/s10800-008-9579-2.

[19] A. Patra, J. Davis, S. Pidaparthy, M.H. Karigerasi, B. Zahiri, A.A. Kulkarni, M.A. Caple, D.P. Shoemaker, J.M. Zuo, P. V. Braun, Electrodeposition of atmosphere-sensitive ternary sodium transition metal oxide films for sodium-based electrochemical energy storage, Proc. Natl. Acad. Sci. U. S. A. 118 (2021) 1–11. https://doi.org/10.1073/pnas.2025044118.